

## Thrombospondin-1 limits ischemic tissue survival by inhibiting nitric oxide-mediated vascular smooth muscle relaxation

Jeff S. Isenberg,<sup>1</sup> Fuminori Hyodo,<sup>2</sup> Ken-Ichiro Matsumoto,<sup>2</sup> Martin J. Romeo,<sup>1</sup> Mones Abu-Asab,<sup>1</sup> Maria Tsokos,<sup>1</sup> Periannan Kuppusamy,<sup>3</sup> David A. Wink,<sup>2</sup> Murali C. Krishna,<sup>2</sup> and David D. Roberts<sup>1</sup>

<sup>1</sup>Laboratory of Pathology and <sup>2</sup>Radiation Biology Branch, Center for Cancer Research, National Cancer Institute, National Institutes of Health, Bethesda, MD;

<sup>3</sup>Davis Heart & Lung Research Institute, Department of Internal Medicine, The Ohio State University, Columbus

**The nitric oxide (NO)/cGMP pathway, by relaxing vascular smooth muscle cells, is a major physiologic regulator of tissue perfusion. We now identify thrombospondin-1 as a potent antagonist of NO for regulating F-actin assembly and myosin light chain phosphorylation in vascular smooth muscle cells. Thrombospondin-1 prevents NO-mediated relaxation of precontracted vascular smooth muscle cells in a collagen matrix. Functional magnetic resonance imaging**

**demonstrated that an NO-mediated increase in skeletal muscle perfusion was enhanced in thrombospondin-1-null relative to wild-type mice, implicating endogenous thrombospondin-1 as a physiologic antagonist of NO-mediated vasodilation. Using a random myocutaneous flap model for ischemic injury, tissue survival was significantly enhanced in thrombospondin-1-null mice. Improved flap survival correlated with increased recovery of oxygen levels in**

**the ischemic tissue of thrombospondin-1-null mice as measured by electron paramagnetic resonance oximetry. These findings demonstrate an important antagonistic relation between NO/cGMP signaling and thrombospondin-1 in vascular smooth muscle cells to regulate vascular tone and tissue perfusion. (Blood. 2007; 109:1945-1952)**

© 2007 by The American Society of Hematology

### Introduction

Tissue ischemia is a major cause of morbidity and mortality associated with cardiovascular disease and diabetes.<sup>1,2</sup> Despite advances in wound closure based on surgical restorations with complex tissue units,<sup>3</sup> many surgical patients experience wound healing complications involving tissue ischemia and necrosis.<sup>4</sup> Patient morbidity resulting from surgical flap necrosis remains a substantial health problem.<sup>5</sup>

Resolution of acute and chronic ischemia requires restoration of tissue perfusion as well as suppressing the inflammatory response triggered by reperfusion. If ischemia is secondary to vascular insufficiency or thrombosis, induction of an angiogenic response may also be required. Treatments to address these factors, including hyperbaric oxygen, intravenous thrombolytics, anti-inflammatory agents, and local application of angiogenesis promoters, have been developed but have yielded only limited success.<sup>6-10</sup>

Nitric oxide (NO) is a key signaling molecule in ischemia. NO stimulates vascular smooth muscle cell (VSMC) relaxation to increase blood flow and tissue perfusion.<sup>11-13</sup> Low-dose NO also has proangiogenic and anti-inflammatory activities.<sup>14-16</sup> Consistent with these activities, elevating NO levels increases tissue survival in situations of ischemic insult.<sup>17</sup>

To improve the effectiveness of NO and other agents for treating ischemia and to understand why such treatments may fail, endogenous inhibitors that may antagonize their activity must be identified. Increased thrombospondin-1 (TSP1) expression during wound healing and following ischemic injury in the heart, kidney, and diabetic limbs suggests a potential role for this protein in the pathogenesis of ischemia.<sup>18-22</sup> The potent antiangiogenic activity of

TSP1 could aggravate ischemia, whereas its anti-inflammatory activity may be beneficial.<sup>23,24</sup>

We recently reported that TSP1 potently inhibits NO/cGMP signaling in endothelial cells and VSMCs.<sup>25,26</sup> Given the central role that this pathway plays in controlling vascular tone,<sup>13,27</sup> these findings suggested that TSP1 may also regulate VSMC contractility, blood vessel diameter, and flow.

Here, we demonstrate that TSP1 antagonizes NO signals to regulate the actin/myosin cytoskeleton and contraction of VSMCs in vitro. We show that endogenous TSP1 modulates acute effects of NO in vivo on tissue perfusion and blood oxygen levels in healthy muscle and in ischemic tissues following surgery. We further show that soft-tissue survival in ischemic myocutaneous flaps is increased in the absence of endogenous TSP1 and that this negative effect of endogenous TSP1 on tissue survival is NO dependent.

### Materials and methods

#### Animals

C57/B16 wild-type (WT) and TSP1-null mice were housed in a pathogen-free environment and had ad libitum access to filtered water and standard rat chow. Handling and care of animals was in compliance with the guidelines established by the Animal Care and Use Committee of the National Cancer Institute and the National Institutes of Health.

#### Cells and reagents

Aortic-derived VSMCs were isolated from WT and TSP1-null mice as previously described<sup>28</sup> and cultured in smooth muscle growth medium.

Submitted August 14, 2006; accepted October 20, 2006. Prepublished online as *Blood* First Edition Paper, November 2, 2006; DOI 10.1182/blood-2006-08-041368.

The online version of this article contains a data supplement.

An Inside *Blood* analysis of this article appears at the front of this issue.

The publication costs of this article were defrayed in part by page charge payment. Therefore, and solely to indicate this fact, this article is hereby marked "advertisement" in accordance with 18 USC section 1734.

© 2007 by The American Society of Hematology

Human aortic VSMCs (HAVSMCs; Cambrex, Walkersville, MD) were maintained in smooth muscle cell growth medium supplemented with the manufacturer's additives (SM-GM; Cambrex) and 2% FCS in 5% CO<sub>2</sub> at 37°C. Cells were used within passages 4 to 9. Monomeric type I collagen was obtained from Inamed (Fremont, CA). *N*-nitro-*L*-arginine methyl ester (L-NAME) and isosorbide dinitrate (ISDN) were purchased from Sigma (St Louis, MO). Lithium phthalocyanine (LiPc) crystals were prepared as previously described.<sup>29,30</sup> Diethylamine NONOate (DEA/NO) and diethyltriamine NONOate (DETA/NO) were kindly provided by Dr Larry Keefer (National Cancer Institute, Frederick, MD). TSP1 was prepared from human platelets obtained from the NIH blood bank as previously described.<sup>31</sup>

### Actin cytoskeleton staining

VSMCs were grown on glass well slides (Lab-Tek; Nunc, Rochester, NY) under standard growth conditions. Cells were incubated at 37°C for 1 hour in serum and additive-deficient growth medium and the indicated treatment agents, after which the media were removed and the cells were fixed in 4% paraformaldehyde in PBS (pH 7.4; Fisher Scientific, Suwanee, GA) for 15 minutes at room temperature. After washing with DPBS, cells were permeabilized for 5 minutes in 0.1% Triton X-100 in PBS and then blocked in M199E/2% BSA for 30 minutes at room temperature. Cells were stained for F-actin with 1 U/200  $\mu$ L medium/1% BSA of Oregon Green 488 phalloidin (Molecular Probes, Carlsbad, CA). Slides were imaged using an Olympus (Center Valley, PA) IX70 microscope and photographed at constant exposure and gain. In other experiments VSMCs were plated on 24-well culture plates (Nunc, Kamstrup, Denmark) in smooth muscle growth medium (50 000 cells/well) and weaned from serum and additives over 24 hours. Cell treatment was performed with the indicated agents in plain medium with 0.1% BSA for 5 minutes. Wells were processed as described for imaging experiments. Following staining with phalloidin, cells were incubated in methanol for 30 minutes, samples were divided into aliquots onto 96-well black plates, and fluorescence was read at 520 nm (excitation 495 nm). Data were normalized to total protein. Results represent the mean plus or minus SD of at least 3 separate experiments.

### 3D matrix contraction assay

Type I collagen gel (3 mg/mL) with 10  $\times$  M199 (Gibco, Grand Island, NY) at a 10:1 ratio of collagen to medium was prepared, pH balanced with NaOH, and seeded with either HAVSMCs (50 000 cells in 75  $\mu$ L gel/well) or VSMCs harvested from aortic segments from C57Bl6 WT or TSP1-null mice (75 000 cells in 75  $\mu$ L gel/well) and divided into aliquots onto 96-well plates (Nunc, Denmark). Plates were incubated for 12 hours at 37°C and 5% CO<sub>2</sub>, allowing for gelation and cell spreading in keeping with published protocols,<sup>32</sup> gently released from the well walls with a sterile 2- $\mu$ L pipette tip, and incubated in serum and additive-deficient growth medium with 0.1% BSA in the presence of the indicated treatment agents for 10 hours. Utilization of the 96-well plate format allowed for multiple replicates of each treatment condition ( $n = 5$ ), which minimized errors because of variability in gel release from the well wall. Increased cell densities were used in experiments conducted with murine primary VSMCs to compensate for increased cell loss on gelation as compared with HAVSMCs. Contraction was determined by measuring the diameter in perpendicular planes ( $x$ ,  $y$ ) of each disk, an average was obtained, and surface area was calculated as  $(d/2)^2\pi$ . Experiments were performed in triplicate. Results represent the mean  $\pm$  SD of at least 3 separate experiments.

### Myosin light chain phosphorylation

VSMCs were plated at 90% confluence and grown in smooth muscle growth media containing 2% FBS overnight. To stimulate MLC phosphorylation, sphingosine-1-phosphate (S1P; Biomol, Plymouth, PA) was added at a final concentration of 100 nM. The nitric oxide donor DEA/NO was added at a final concentration of 10  $\mu$ M. For TSP1 pretreatment, cells were incubated with 2.2 nM TSP1 before the addition of S1P or DEA/NO. Cells were subsequently washed twice with PBS and lysed immediately in 1  $\times$  SDS sample buffer containing 10  $\mu$ g/mL leupeptin, 10  $\mu$ g/mL aprotinin,

1 mM Na<sub>3</sub>VO<sub>4</sub>, and 40 mM NaF. Lysates prepared in the SDS sample buffer were electrophoresed in 4% to 12% BisTris NuPAGE gels and transferred to PVDF membranes prior to immunoblotting with rabbit polyclonal antibodies against myosin light chain-2 (MLC2) and phospho-MLC2 (T18/S19; Cell Signaling Technology, Danvers, MA).

### Flap model

WT and TSP1-null mice were matched for sex and age. Under isoflurane inhalation anesthesia 1  $\times$  2 cm random myocutaneous flaps were raised. Where indicated, animals received either L-NAME (0.5 mg/mL) or ISDN (1 mg/mL) ad libitum in drinking water during the postoperative period. On postoperative day 7, the animals were again anesthetized with inhalation of isoflurane, and flaps were evaluated. Viable and necrotic areas of the flaps were determined by color, refill, eschar, and the pin-prick test. Outlines of viable and nonviable areas were traced using transparent film, and the area of flap necrosis versus total flap area was determined as described.<sup>33</sup>

### Histology

Sections of excised wounds were cut parallel to the long axis of each flap, including the entire length of the tissue sample, fixed in 10% buffered formaldehyde, paraffin embedded, and sectioned at a thickness of 5  $\mu$ m. Sections were then stained with hematoxylin and eosin (H + E) according to standard procedures. Review of each slide was performed by an independent pathologist blinded to the origin of each tissue slide. Other tissue sections from wild-type animals were stained for immunohistochemistry.

### Immunohistochemistry

Immunohistochemical studies were performed on 5- $\mu$ m-thick paraffin-embedded tissue sections from flaps harvested at 4 and 72 hours. Sections were deparaffinized in xylene and rehydrated in graded alcohol (100%, 95%, and 70%). Sections were subjected to antigen retrieval solution in a pressure cooker containing 1.5 L antigen retrieval solution, pH 6.1 (Dako, Carpinteria, CA) for 10 minutes, cooled down in the same solution for 20 minutes at room temperature, and then washed with PBS 1  $\times$ . Block activity of endogenous peroxidase and secondary antibody were performed using EnVision plus System-HRP (DAB) antimouse (Dako), 5 and 30 minutes, respectively, at room temperature. A blocking step was performed using Protein Block Serum-Free (Dako) for 10 minutes. The TSP1 primary antibody (clone A6.1; NeoMarkers, Fremont, CA) was applied for 1 hour at room temperature, and the working dilution was 1:25. The peroxidase reaction was developed with 3,3'-diaminobenzidine chromogen solution (Dako) for 5 minutes. As negative control we used slides that excluded the primary antibody. Only cytoplasmic and extracellular matrix immunoreactivity was considered positive for TSP1. Inflammatory cells were considered as an internal positive control.

### Blood oxygen level-dependent (BOLD) magnetic resonance imaging (MRI)

Magnetic resonance images were acquired using a Bruker Biospin 4.7 T scanner (Bruker BioSpin, Karlsruhe, Germany) and isoflurane anesthesia. Muscle tissue scanned was at rest, so alterations in oxygenation reflected changes in perfusion rather than in oxygen consumption.<sup>34,35</sup> MR measurements were started after the mouse's body temperature reached 37°C. Prior to the experiments, gradient echo-based T<sub>1</sub> sequence was used to determine the target slice location. A series of T<sub>2</sub>\* weighted gradient echo blood oxygenation level dependent (BOLD) image data sets at transverse to the midpoint of the femur were repeatedly acquired for 30 minutes to monitor temporal changes in blood oxygenation and blood flow. DEA/NO (100 nmol/g body weight) was injected with saline via the rectal cannula 5.0 minutes after starting the scan. Imaging parameters used were as follows: TR, 450 ms; Flip angle, 45; Nex, 1; slice thickness, 2 mm; matrix size, 64  $\times$  64; total imaging time for the series was 29 minutes.

### Implantation of LiPc crystals

WT or TSP1-null mice matched for age and sex were anesthetized by administering 1.5% to 2% isoflurane in medical air (flow rate was

700 mL/minutes). The fur of the back was removed by shaving and depilatory cream. A portion of LiPc crystals (5–10 mg) was suspended with an appropriate volume (10–20  $\mu$ L) of corn oil and kneaded until a slurry paste was obtained.<sup>30</sup> Then, the LiPc slurry was placed in the 2- to 3-mm tip of a 20-gauge injection needle. The needle was injected into the desired region of the animal, and the LiPc crystals were pushed out using a smooth-fitting piston. The average weight of the LiPc injected was 0.8 mg. Implantation of LiPc crystal slurry was done to the following 3 locations on the back of the mouse: to the distal and proximal regions of the flap and to an area 1 cm from the flap base.

### EPR measurement of tissue oxygen in vivo

Dorsal modified McFarlane flaps bearing LiPc crystals implanted 7 days prior were created as described above, and electron paramagnetic spin resonance (EPR) measurements were carried out at 3, 6, 24, 48, and 72 hours after the surgical procedure. Again, mice were anesthetized with 1.5% to 2% isoflurane in medical air flow (700 mL/minutes) and placed in a special mouse holder. The surface coil (7.3-mm internal diameter) was placed on the region where the LiPc crystal was implanted. The EPR signal was measured by continuous wave (CW) EPR at 700 MHz using a single-loop surface coil resonator (7.3-mm internal diameter). The 300-MHz CW EPR system, which was previously described,<sup>30,36</sup> was equipped with a 700-MHz bridge and the surface coil-type resonator, instead of a 300-MHz bridge and a parallel coil-type resonator. The experimental settings were as follows: microwave frequency, 700 MHz; scan rate, 0.5 Gauss/second; and time constant, 0.003 second; field modulation frequency, 13.5 kHz. The microwave power (0.08–0.3 mW) and field modulation width (0.01–0.2 Gauss) were adjusted to avoid saturation and line broadening. The core body temperature (sampled continuously from the rectum) was monitored by a nonmagnetic probe (FISO Technologies, Quebec, Canada) and was kept at  $37^{\circ}\text{C} \pm 0.5^{\circ}\text{C}$  using a hot air heater during EPR measurements. Tissue  $\text{pO}_2$  values were calculated from a calibration curve obtained previously for each batch of LiPc crystals used in the experiment.

### Statistics

All experiments were replicated at least 3 times. Results are presented as the mean plus or minus SD with analysis of significance done by the Student *t* test or one-way or 2-way ANOVA with Tukey post hoc test where indicated using Origin software (version 7; OriginLabs, Northhampton, MA), with significance taken at *P* values less than .05.

## Results

### TSP1 inhibits NO-induced actin disassembly in VSMCs

Actin cytoskeletal reorganization and actin-myosin interactions control the contractile state of VSMCs.<sup>37</sup> Treatment of human aortic VSMCs (HAVSMCs) with exogenous NO resulted in dissolution of organized actin bundles and decreased total cellular F-actin (Figure 1A–B,E). Based on inhibition of actin disassembly by NO in the presence of 1H-[1,2,4]oxadiazole[4,3-a]quinoxalin-1-one, this activity of NO requires soluble guanylyl cyclase (Figure S1I–J, available on the *Blood* website; see the Supplemental Figures link at the top of the online article). TSP1 blocks NO-induced changes in actin organization in endothelial cells.<sup>25</sup> Similarly, the addition of TSP1 alone to VSMCs slightly increased F-actin levels (Figure 1C,E) and completely prevented actin disassembly by NO (Figure 1D–E). S1P, a lipid known to regulate VSMC contractility (reviewed in Watterson et al<sup>38</sup>), also increased F-actin, which was disassembled on the addition of NO (Figure 1E; Figure S1E–F). Addition of TSP1 further increased F-actin in the presence of S1P. However, disassembly of S1P-induced F-actin by NO was attenuated in the presence of TSP1 (Figure 1E; Figure S1G–H).

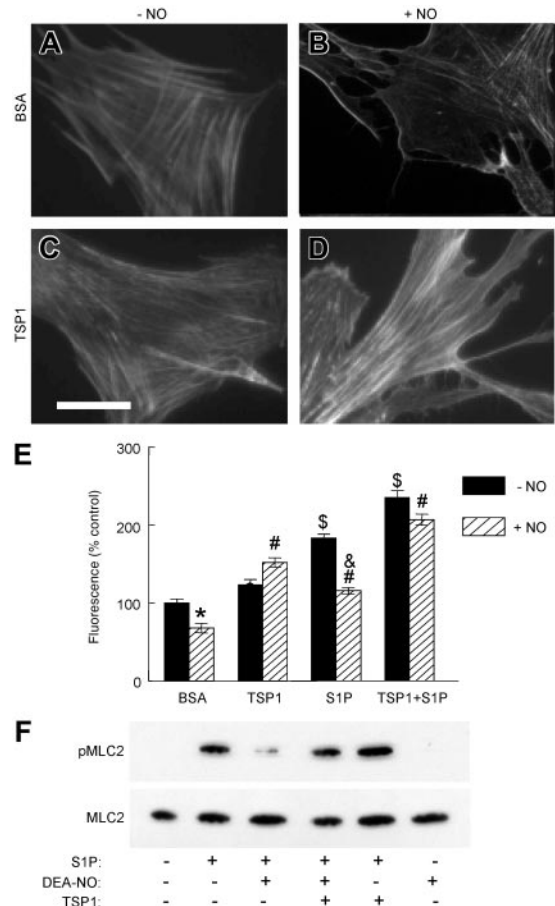


**Figure 1. TSP1 antagonizes NO-dependent alterations in F-actin and dephosphorylation of MLC in VSMCs.** HAVSMCs plated on glass chamber slides were incubated in basal medium with 0.1% BSA (A–B) or 2.2 nM TSP1 (C–D)  $\pm$  DEA/NO (10  $\mu$ M). Cells were then fixed, permeabilized, and stained with Oregon Green-phalloidin to visualize F-actin. Photomicrographic images were acquired on a Nikon Eclipse E1000 microscope (Nikon, Melville, NY) using a Plan Apo objective lens. Low-magnification images were taken at 20 $\times$  and a numeric aperture of 0.75; high-power images, at 40 $\times$  and a numeric aperture of 0.95. No imaging medium or solution was used. A Cool Snap FX camera (Roberts Scientific, Tucson, AZ), IP Lab 3.5 software (Scanalytics, Fairfax, VA), and Photoshop CS (Adobe Systems, San Jose, CA) were used for image acquisition and processing. Photomicrographs representative of 3 separate experiments are presented. Scale bar = 50  $\mu$ m. HAVSMCs in 96-well plates were similarly treated and stained, and the fluorescence was signal quantified (E). \**P* < .05 versus BSA – NO, Student *t* test. #*P* < .05 versus BSA + NO, \$*P* < .05 versus BSA – NO, 2-way ANOVA. &*P* < .05 versus S1P – NO, one-way ANOVA. Lysates of HAVSMCs in growth medium with 2% serum and treated with the indicated combinations of 100 nM S1P, 10  $\mu$ M DEA/NO, and 2.2 nM TSP1 for 5 minutes were separated by SDS–polyacrylamide gel electrophoresis (PAGE) and analyzed by Western blot to determine the levels of MLC phosphorylation and total MLC (F). The blot shown is representative of 4 independent experiments. Results are presented as the mean  $\pm$  SD.

### Myosin light chain-2 dephosphorylation induced by NO is blocked by TSP1

MLC phosphorylation is a critical step in VSMC contraction.<sup>37</sup> S1P inhibits MLC phosphatase via Rho and thereby increases phosphorylation of MLC.<sup>39</sup> This response to S1P was reversed by exogenous NO (Figure 1F). Concurrent treatment with exogenous TSP1 prevented this activity of NO and partially restored MLC phosphorylation.

### Exogenous and endogenous TSP1 inhibit NO-stimulated VSMC relaxation

Blood flow is controlled by vascular resistance, which depends on blood vessel diameter regulated by contraction and relaxation of VSMCs. The

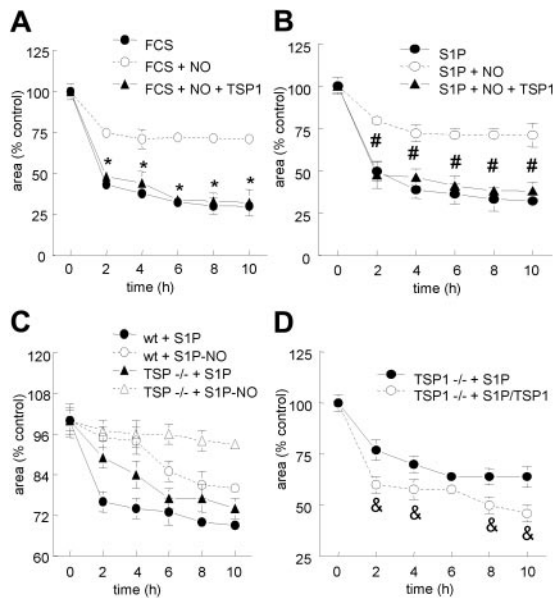


**Figure 2. NO-stimulated VSMC contraction is blocked in the presence of exogenous and endogenous TSP1 and S1P.** Type I collagen gels (3 mg/mL) were prepared and seeded with either HAVSMCs (A-B) (50 000 cells in 75  $\mu$ L gel/well) or VSMCs harvested from aortic segments from WT or TSP1-null mice (C-D) (75 000 cells in 75  $\mu$ L gel/well) and divided into aliquots in 96-well plates (Nunc, Denmark) and incubated overnight. Wells treated with TSP1 were preincubated overnight with 2.2 nM TSP1. Following release of the gels, contraction was initiated with either 10% FCS or 100 nM S1P  $\pm$  10  $\mu$ M DETA/NO, and contraction was determined. \* $P$  < .05 versus FCS + NO, # $P$  < .05 versus S1P + NO, & $P$  < .05 versus TSP  $\pm$  S1P, Student  $t$  test. Results are presented as the mean  $\pm$  SD.

effects of TSP1 on NO-mediated changes in F-actin and MLC phosphorylation suggested that TSP1 may regulate VSMC contraction. Using a well-characterized assay of VSMC contraction in 3D type I collagen gels,<sup>32</sup> HAVSMCs demonstrated significant contraction in response to either 10% FCS or 100 nM S1P, a component of serum and stimulator of VSMC contraction<sup>40</sup> (Figure 2A-B). Treatment with a slow-releasing NO donor (DETA/NO) inhibited gel contraction by both agonists, but the addition of 2.2 nM TSP1 completely abrogated this inhibitory activity of NO (Figure 2A-B). Conversely, aortic-derived TSP1-null murine VSMCs demonstrated reduced contraction to S1P compared with WT cells, although both were relaxed by NO (Figure 2C). A positive effect of TSP1 on the contractile response to S1P was confirmed by adding exogenous

TSP1, which increased the contractile response of TSP1-null cells to S1P (Figure 2D). A more modest enhancement of S1P-induced contraction was observed for WT cells (results not shown). The direct effect of TSP1 on S1P-induced contraction may result from cGMP-dependent activation of the MLC phosphatase,<sup>39</sup> which should be higher in TSP1-null cells because of their elevated basal cGMP levels.<sup>26</sup>

**Endogenous TSP1 limits NO-stimulated soft-tissue perfusion**

A major physiologic function of NO is to control tissue perfusion by regulating vascular smooth muscle tone.<sup>27</sup> To investigate whether endogenous TSP1 regulates this vascular response to exogenous NO, we used BOLD MRI<sup>34,41</sup> for real-time imaging of blood oxygenation in WT and TSP1-null C57Bl6 mice (Figure 3). Intrarectal injection of the rapidly releasing NO donor DEA/NO ( $t_{1/2}$ , ~ 2 minutes) induced rapid focal increases in the BOLD MRI signal in lateral thigh sections of both TSP1-null and WT mice (Figure 3A-B). Notably, the magnitude of this signal in areas showing a positive response to NO was significantly greater in TSP1-null mice (25%) than in WT mice (15%; Figure 3C;  $P$  < .05). Furthermore, the rate of signal change was greater in the null animals versus WT animals. In contrast, areas with decreased BOLD signal did not differ significantly (TSP null, -14%; WT, -11%). Therefore, endogenous TSP1 significantly limits the acute vasodilator response to NO in skeletal muscle tissue.

**Endogenous TSP1 limits random myocutaneous flap survival**

Tissue survival following a fixed ischemic insult requires restoration of regional perfusion and blood flow. We used a well-characterized model of soft-tissue ischemic responses<sup>42</sup> to assess the role of endogenous TSP1 in tissue survival under ischemic stress. WT and TSP1-null mice matched for sex and age underwent random dorsal modified McFarlane flap elevation and suturing under inhalation anesthesia (Figure S2). Changes in flap perfusion and viability were noticeable immediately after surgical elevation in WT animals, with the distal aspects of flaps appearing pale and hypoperfused. On postoperative day 7, flaps in WT animals demonstrated 38% less tissue survival compared with flaps in TSP1-null animals (59%  $\pm$  6% versus 96%  $\pm$  2%,  $P$  < .05; Figure 4A,D). Flap survival was not sex dependent. Older WT mice (> 6 months) tended to experience greater tissue loss compared with

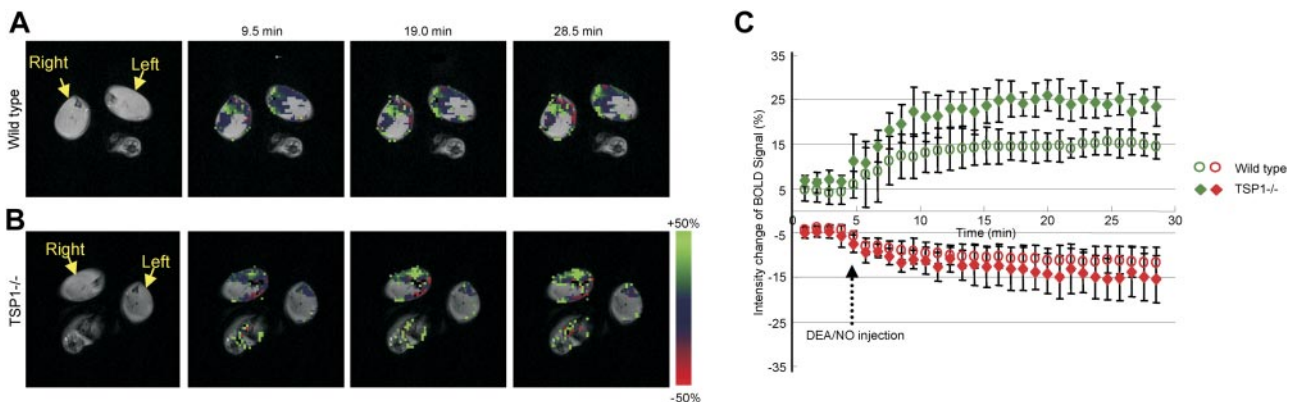


**Figure 3. Endogenous TSP1 limits tissue perfusion responses to NO in vivo.** BOLD MRI images for (A) WT and (B) TSP1-null mice were obtained from  $T_2^*$  weighted sequences. DEA/NO (100 nmol/g body weight) was injected with saline via an intrarectal cannula 5 minutes after starting the scan. Green and red colors show positive and negative BOLD MRI signals, respectively, at the indicated times after NO administration. The BOLD images were superimposed with the corresponding anatomic images to determine exact locations in the lateral thigh sections. (C) BOLD MRI signal changes as a function of time after NO challenge. The green and red plots show increased and decreased BOLD MRI signals, respectively. Values are presented as mean  $\pm$  SD from 5 and 4 experiments in WT and TSP1-null mice, respectively.

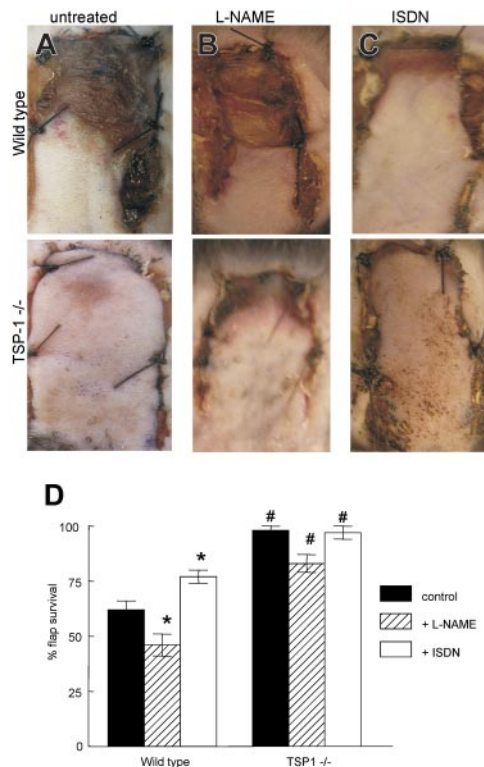


**Figure 4. Endogenous TSP1 and NO modulate tissue survival under ischemic conditions.** (A) Representative random flaps were photographed 7 days following surgery for untreated WT and TSP1-null mice, WT and TSP1-null mice receiving L-NAME (500 mg/L; B), or mice receiving ISDN (1 mg/mL; C) in the drinking water during the postoperative period. (D) Flap survival is expressed as the percentage of the total involved area. Results are the mean  $\pm$  SD of 24 animals (12 age- and sex-matched pairs) of untreated WT and TSP1-null mice, 16 animals (8 matched pairs) treated with L-NAME, and 16 animals (8 matched pairs) treated with ISDN. \* $P < .05$  versus control, one-way ANOVA. # $P < .05$  versus wild type, 2-way ANOVA.

younger animals (10-16 weeks), but this difference was not statistically significant.

#### Postoperative inhibition of nitric oxide synthase (NOS) increases tissue necrosis

To address the role of NO signaling in random soft-tissue flap survival, WT and TSP1-null mice were given ad libitum access to drinking water containing L-NAME (0.5 mg/mL) during the postoperative period. In WT animals, NOS inhibition by L-NAME significantly decreased mean flap survival ( $46\% \pm 2\%$ ) compared with flaps in animals that did not receive L-NAME (Figure 4B,D;  $P < .05$ ). In contrast, NOS inhibition by L-NAME moderately increased tissue necrosis in TSP1-null animals ( $82\% \pm 4\%$  survival) but did not reach statistical significance.

#### An NO donor decreases tissue necrosis in random soft-tissue flaps in WT mice

To increase tissue NO levels, animals were provided ISDN (1 mg/mL) in their drinking water during the postoperative period. Flap survival was increased significantly in the treated WT animals compared with untreated WT animals ( $79\% \pm 4\%$  versus  $59\% \pm 6\%$ ;  $P < .05$ ; Figure 4C-D). ISDN treatment resulted in essentially complete flap survival in TSP1-null animals compared with untreated animals, but the increase was not significant ( $100\% \pm 3\%$  versus  $97\% \pm 2\%$ ). Therefore, exogenous NO can partially overcome the inhibitory effect of endogenous TSP1 on ischemic tissue survival.

#### TSP1-null flaps exhibit increased granulation tissue

Histologic examination of excised flaps demonstrated that granulation tissue formation at the necrotic tissue sites and the interface between viable and necrotic tissue was significantly higher in the flaps of time-matched TSP1-null versus WT mice (Figure 5A-B). Consistent with the known antiangiogenic activity of TSP1, the granulation tissue in the TSP1 null flaps contained a larger number of newly formed capillaries when compared with that of the WT mice (Figure 5C-D).

Immunohistochemical staining with a TSP1 antibody of sections from wild-type McFarlane flaps at 4 hours after surgery showed diffuse TSP1 staining, including the epidermis, subcutaneous blood vessels, extracellular matrix, striated muscle, and inflammatory cells (Figure 5E). By 72 hours, TSP1 staining had localized to the margins of the striated muscle cell component of the flap and surrounding extracellular matrix (Figure 5F). Differences in the degree of TSP1 staining in proximal versus distal regions of flaps could not be discerned.

#### Endogenous TSP1 acutely and chronically alters postsurgery tissue $pO_2$

Recovery and maintenance of tissue oxygenation are critical for tissue survival following ischemic injury. EPR was used to determine tissue  $pO_2$ , sensed by line broadening of LiPc crystals preimplanted in proximal and distal regions of dorsal flaps and in a unit of soft tissue adjacent to the flap (control; Figure 6A).

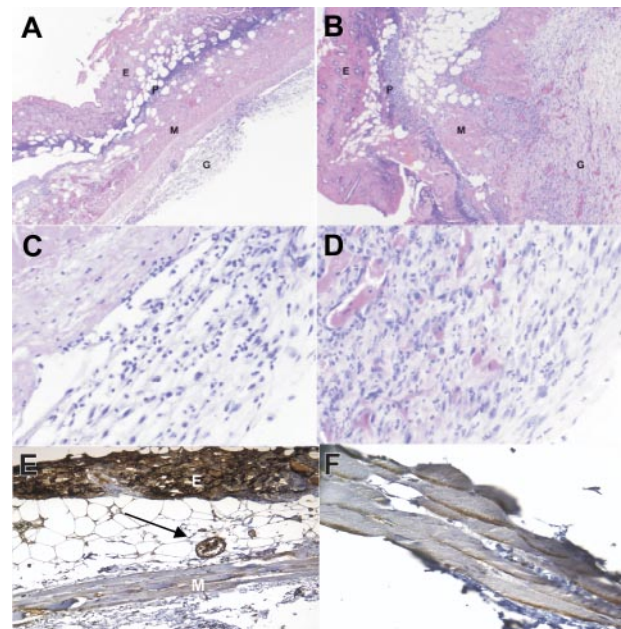


**Figure 5. Increased angiogenic and spindle cell responses in random ischemic flaps in the absence of endogenous TSP1.** Sections from necrotic areas of the excised skin flap in WT (A) and TSP1-null (B) mice are shown. In WT mice the epidermis (E) is necrotic and heavily infiltrated by polymorphonuclear leukocytes (P). A layer of loose granulation tissue (G) is present under the muscular layer (M). The layer of granulation tissue is significantly thicker and more heavily vascularized in the skin flap of the TSP1-null mouse. H + E; original magnification,  $\times 4$ . Higher magnification of the granulation tissue in the WT (C) and TSP1-null (D) flaps shows more prominent spindle-cell proliferation and capillary formation in the TSP1-null flap. H + E; original magnification,  $\times 20$ . Immunohistochemical staining with a TSP1 monoclonal antibody of wild-type flaps at 4 hours (E) and 72 hours (F) after surgery was performed. Tissue obtained 4 hours after surgery demonstrated diffuse TSP1 staining of the epidermis, subcutaneous arterioles (arrow), extracellular matrix, striated muscle, and inflammatory cells. At 72 hours after surgery staining was localized to muscle cell borders and extracellular matrix with less staining in other areas. Original magnification,  $\times 20$ .

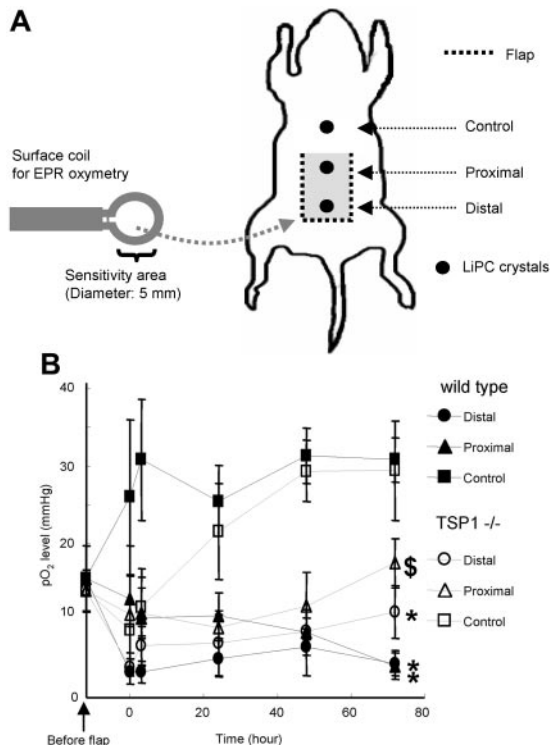


**Figure 6. Tissue pO<sub>2</sub> in WT and TSP1-null mice after flap treatment using EPR oxymetry.** (A) Schematic showing LiPc crystal placement in relation to a dorsal random myocutaneous flap. LiPc crystals were implanted in the dorsal subdermal area of mice 7 days prior to flap elevation. Initial measurements were performed by 700-MHz EPR spectroscopy with a small surface coil to confirm crystal location and calculate basal pO<sub>2</sub> levels. Body temperature of the animals was maintained at 37.5°C ± 0.5°C. Following flap elevation and suturing, measurements were recorded at the indicated times (B). Data represent the mean ± SE of measurements from 4 animals in each group. \$P < .05 between proximal and distal against control in WT versus TSP1<sup>-/-</sup>. \*P < .05 between proximal and distal.

Preoperative tissue pO<sub>2</sub> values obtained 1 hour prior to flap elevation were essentially identical in WT and TSP1-null mice (Figure 6B). Immediately following surgery, tissue pO<sub>2</sub> in the control area adjacent to the flap increased rapidly in WT mice, presumably because of acute inflammatory responses associated with the adjacent injury. The elevated pO<sub>2</sub> in the control area was maintained for at least 3 days. Remarkably, this acute response was initially absent in the control areas of TSP1-null mice, but their pO<sub>2</sub> gradually increased to match the WT control pO<sub>2</sub> at 48 hours.

As expected, pO<sub>2</sub> values within the flaps decreased immediately following surgery to similar levels for TSP1-null and WT mice (Figure 6B). In WT animals, tissue pO<sub>2</sub> in the distal and proximal flap areas remained low 3 days following surgery, being 4.5 ± 1.6 mm Hg and 4.2 ± 1.7 mm Hg, respectively. Conversely, pO<sub>2</sub> values in distal and proximal area of flaps for TSP1-null mice showed a progressive recovery of tissue pO<sub>2</sub> with time. The pO<sub>2</sub> values of distal and proximal flap areas in TSP1-null animals 3 days after surgery were significantly greater (11.1 ± 3.4 mm Hg and 17.5 ± 3.2 mm Hg, respectively; P < .05) than pO<sub>2</sub> found in WT flaps.

## Discussion

TSP1 potently antagonizes the adhesive, migratory, and proliferative responses of endothelial and VSMCs to NO by limiting cGMP signaling.<sup>25,26</sup> The same NO signaling pathway is important for

maintaining vascular patency through relaxing VSMCs, which causes blood vessel dilation and increased tissue perfusion.<sup>43</sup> We now identify TSP1 as a potent physiologic antagonist of NO signaling to regulate VSMC cytoskeletal and contractile responses in vitro and tissue perfusion in vivo.

Calcium binding to calmodulin activates MLC kinase to phosphorylate MLC. Phosphorylated MLC stimulates interactions between myosin and actin, cross-bridge cycling, and ultimately cell contraction. S1P induces VSMC contraction via several S1P receptors, which in turn signal to inhibit MLC phosphatase activity.<sup>39</sup> NO/cGMP signaling relaxes VSMCs via cGMP-dependent protein kinase, which enhances intracellular calcium [Ca<sup>2+</sup>]<sub>i</sub> sequestration and also regulates MLC phosphatase.<sup>39</sup> Consistent with these signaling pathways, MLC phosphorylation in VSMCs is increased by S1P, and NO blocks this response. Significantly, TSP1 prevents the NO-driven dephosphorylation of MLC in S1P-treated VSMCs. The activity of TSP1 to antagonize NO-driven actin disassembly is also important because F-actin-containing cytoskeletal stress fibers interact with the contractile protein myosin to mediate VSMC contraction. These results predicted that TSP1 should block NO-driven relaxation of VSMCs, which was confirmed using in vitro assays of VSMC contraction mediated by serum or S1P in 3D collagen gels.

The differential effects of an NO donor on blood flow in WT and TSP1-null mice confirm the physiologic significance of TSP1 as an antagonist of NO-mediated vasorelaxation. In resting animals, the changes in blood oxygen levels detected by BOLD MRI directly reflect alterations in tissue blood flow. Using this technique, we found that endogenous TSP1 limits the increase in peripheral blood oxygenation following an acute NO challenge. The speed of this response supports our hypothesis that preexisting endogenous TSP1 limits soft-tissue perfusion by inhibiting NO-mediated vasorelaxation.

Results from the ischemic flap model indicate a clinically important role for TSP1 in modulating tissue perfusion. Tissue survival following a fixed ischemic insult was markedly increased in the absence of endogenous TSP1. Importantly, the negative effect of endogenous TSP1 on tissue survival could be partially overcome by providing exogenous NO. Recent clinical reports suggest immediate relevance of the present findings to human disease. Increased TSP1 expression in ischemic lower extremities correlates with limb amputation rates.<sup>19</sup> In addition, TSP1 has been ascribed a role in myocardial infarct size, although the mechanism behind its effects remains debated.<sup>20,21</sup> In the absence of TSP1, inflammatory responses were increased and associated with greater infarct remodeling, although total infarct size did not differ between control and TSP1-null animals.<sup>21</sup> Furthermore, TSP1 expression was rapidly induced following reperfusion after ischemic injury in the kidney, and exogenous TSP1 induced proximal tubule injury.<sup>22</sup> These reports provide evidence that TSP1 influences tissue preservation under ischemic conditions through different, although not mutually exclusive, mechanisms.

Conversely, NO clearly plays an important role in modulating tissue ischemia secondary to vascular insufficiency. In both random flap and ischemia/reperfusion models, exogenous NO and L-arginine, the substrate of NOS, are tissue protective.<sup>44</sup> Treatment with L-arginine in the drinking water and autologous bone marrow cells increased perfusion in a hind-limb ischemia model.<sup>45</sup> Non-selectively inhibiting NOS using L-NAME decreased tissue preservation under ischemic conditions,<sup>46</sup> and eNOS-null mice have defective recovery of blood flow following hind-limb ischemia.<sup>47</sup> These results are consistent with the effects of

L-NAME to decrease and ISDN to increase tissue survival in our ischemic flap model.

LiPc EPR provides a complementary assessment of pO<sub>2</sub> in ischemic soft-tissue flaps.<sup>29,30</sup> At 2 anatomic locations, tissue pO<sub>2</sub> after 3 days was greater in TSP1-null flaps as compared with WT flaps. These results correlate with the significantly greater tissue survival under fixed ischemic stress in TSP1-null flaps. Limiting NO production by inhibiting NOS increased, whereas supplementing NO using ISDN decreased tissue necrosis only in WT mice, further supporting a role for TSP1 in limiting the alteration of tissue perfusion by NO.

The immediate divergence in pO<sub>2</sub> following surgery in areas adjacent to null versus WT flaps indicates that endogenous TSP1 also acutely regulates tissue pO<sub>2</sub> under ischemic stress. This positive effect of endogenous TSP1 on pO<sub>2</sub> cannot be directly explained by the negative effect of TSP1 on vasodilation reported here. However, the delayed increase in TSP1-null mice might result from the reported defect in monocyte recruitment noted previously in excisional skin wounds.<sup>48</sup> In this case, the immediate increase in pO<sub>2</sub> in the WT mice could result from inflammatory cytokine release by macrophages recruited to the area adjacent to the flap in a TSP1-dependent manner.

The present studies extend the known activity of TSP1 as a potent antagonist of NO-induced vascular cell adhesion, proliferation, and migration<sup>25,26</sup> to modulation of NO-dependent VSMC contractility and MLC phosphorylation. Endogenous TSP1 thereby directly limits NO-mediated increases in perfusion of healthy and injured tissues. Thus, TSP1 plays a broader role in regulating vascular physiology than previously known, and drugs developed to mimic the antiangiogenic activity of TSP1<sup>49</sup> may likewise have

antivasodilator activities that impact their clinical use. Conversely, inhibiting TSP1 expression or function could improve clinical outcome for surgical procedures that result in ischemic stress.

## Acknowledgments

We thank Dr Jack Lawler for providing mice and Dr Larry Keefer for providing DEA/NO and DETA/NO. We thank Dr Susana Galli for assistance with interpretation of immunostaining.

This work was supported by the Intramural Research Program of the National Institutes of Health, National Cancer Institute, Center for Cancer Research (M.T., D.A.W., M.C.K., and D.D.R.).

## Authorship

Contribution: J.S.I. designed and performed the in vitro and in vivo experiments as well as EPR oximetry, collected and interpreted the data, and wrote the manuscript; F.H., K.-I.M., and P.K. performed and interpreted the MRI imaging and EPR oximetry; M.J.R. designed, performed, and interpreted the Western blots; M.A.-A. and M.T. prepared, reviewed, and interpreted the histologic sections; and D.A.W., M.C.K., and D.D.R. designed and interpreted the experiments and wrote the manuscript.

Conflict-of-interest disclosure: The authors declare no competing financial interests.

Correspondence: David D. Roberts, National Institutes of Health, Bldg 10, Rm 2A33, Bethesda, MD 20892-1500; e-mail: droberts@helix.nih.gov.

## References

- Brevetti G, Chiariello M. Peripheral arterial disease: the magnitude of the problem and its socio-economic impact. *Curr Drug Targets Cardiovasc Haematol Disord*. 2004;4:199-208.
- Strandness DE Jr, Eidt JF. Peripheral vascular disease. *Circulation*. 2000;102:IV46-IV51.
- Heller L, Levin LS. Lower extremity microsurgical reconstruction. *Plast Reconstr Surg*. 2001;108:1029-1041; quiz 1042.
- Kuwahara M, Tada H, Mashiba K, et al. Mortality and recurrence rate after pressure ulcer operation for elderly long-term bedridden patients. *Ann Plast Surg*. 2005;54:629-632.
- Castelli ML, Pecorari G, Succo G, Bena A, Andreis M, Sartoris A. Pectoralis major myocutaneous flap: analysis of complications in difficult patients. *Eur Arch Otorhinolaryngol*. 2001;258:542-545.
- Weinzwieg N, Gonzalez M. Free tissue failure is not an all-or-none phenomenon. *Plast Reconstr Surg*. 1995;96:648-660.
- Kubo T, Yano K, Hosokawa K. Management of flaps with compromised venous outflow in head and neck microsurgical reconstruction. *Microsurgery*. 2002;22:391-395.
- Ribuffo D, Chiummariello S, Cigna E, Scuderi N. Salvage of a free flap after late total thrombosis of the flap and revascularisation. *Scand J Plast Reconstr Surg Hand Surg*. 2004;38:50-52.
- Murthy P, Riesberg MV, Hart S, et al. Efficacy of perioperative thromboprophylactic agents in the maintenance of anastomotic patency and survival of rat microvascular free groin flaps. *Otolaryngol Head Neck Surg*. 2003;129:176-182.
- Aronow WS. Management of peripheral arterial disease. *Cardiol Rev*. 2005;13:61-68.
- Moncada S, Higgs A. The L-arginine-nitric oxide pathway. *N Engl J Med*. 1993;329:2002-2012.
- Murad F. Cyclic GMP: synthesis, metabolism, and function: introduction and some historical comments. *Adv Pharmacol*. 1994;26:1-5.
- Ignarro LJ. Biological actions and properties of endothelium-derived nitric oxide formed and released from artery and vein. *Circ Res*. 1989;65:1-21.
- Cooke JP. NO and angiogenesis. *Atheroscler Suppl*. 2003;4:53-60.
- Morbidelli L, Donnini S, Ziche M. Role of nitric oxide in the modulation of angiogenesis. *Curr Pharm Des*. 2003;9:521-530.
- Higuchi H, Granger DN, Saito H, Kurose I. Assay of antioxidant and antiinflammatory activity of nitric oxide in vivo. *Methods Enzymol*. 1999;301:424-436.
- Topp SG, Zhang F, Chatterjee T, Lineaweaver WC. Role of nitric oxide in surgical flap survival. *J Am Coll Surg*. 2005;201:628-639.
- Armstrong LC, Bornstein P. Thrombospondins 1 and 2 function as inhibitors of angiogenesis. *Matrix Biol*. 2003;22:63-71.
- Favier J, Germain S, Emmerich J, Corvol P, Gasc JM. Critical overexpression of thrombospondin 1 in chronic leg ischaemia. *J Pathol*. 2005;207:358-366.
- Sezaki S, Hirohata S, Iwabu A, et al. Thrombospondin-1 is induced in rat myocardial infarction and its induction is accelerated by ischemia/reperfusion. *Exp Biol Med (Maywood)*. 2005;230:621-630.
- Frangiogiannis NG, Ren G, Dewald O, et al. Critical role of endogenous thrombospondin-1 in preventing expansion of healing myocardial infarcts. *Circulation*. 2005;111:2935-2942.
- Thakar CV, Zahedi K, Revelo MP, et al. Identification of thrombospondin 1 (TSP-1) as a novel mediator of cell injury in kidney ischemia. *J Clin Invest*. 2005;115:3451-3459.
- Lawler J. Thrombospondin-1 as an endogenous inhibitor of angiogenesis and tumor growth. *J Cell Mol Med*. 2002;6:1-12.
- Kuznetsova SA, Roberts DD. Functional regulation of T lymphocytes by modulatory extracellular matrix proteins. *Int J Biochem Cell Biol*. 2004;36:1126-1134.
- Isenberg JS, Ridnour LA, Perruccio EM, Espey MG, Wink DA, Roberts DD. Thrombospondin-1 inhibits endothelial cell responses to nitric oxide in a cGMP-dependent manner. *Proc Natl Acad Sci U S A*. 2005;102:13141-13146.
- Isenberg JS, Wink DA, Roberts DD. Thrombospondin-1 antagonizes nitric oxide-stimulated vascular smooth muscle cell responses. *Cardiovasc Res*. 2006;71:785-793.
- Ignarro LJ. Nitric oxide as a unique signaling molecule in the vascular system: a historical overview. *J Physiol Pharmacol*. 2002;53:503-514.
- Isenberg JS, Calzada MJ, Zhou L, et al. Endogenous thrombospondin-1 is not necessary for proliferation but is permissive for vascular smooth muscle cell responses to platelet-derived growth factor. *Matrix Biol*. 2005;24:110-123.
- Afeworki M, Miller NR, Devasahayam N, et al. Preparation and EPR studies of lithium phthalocyanine radical as an oxymetric probe. *Free Radic Biol Med*. 1998;25:72-78.
- Matsumoto A, Matsumoto S, Sowers AL, et al. Absolute oxygen tension (pO<sub>2</sub>) in murine fatty and muscle tissue as determined by EPR. *Magn Reson Med*. 2005;54:1530-1535.
- Roberts DD, Cashel J, Guo N. Purification of thrombospondin from human platelets. *J Tissue Cult Methods*. 1994;16:217-222.
- Li S, Moon JJ, Miao H, et al. Signal transduction in matrix contraction and the migration of vascular smooth muscle cells in three-dimensional matrix. *J Vasc Res*. 2003;40:378-388.

33. Ueda K, Nozawa M, Miyasaka M, Akamatsu J, Tajima S. Sulfatide protects rat skin flaps against ischemia-reperfusion injury. *J Surg Res.* 1998;80:200-204.
34. Krishna MC, Devasahayam N, Cook JA, Subramanian S, Kuppusamy P, Mitchell JB. Electron paramagnetic resonance for small animal imaging applications. *ILAR J.* 2001;42:209-218.
35. Noseworthy MD, Bulte DP, Alfonsi J. BOLD magnetic resonance imaging of skeletal muscle. *Semin Musculoskelet Radiol.* 2003;7:307-315.
36. Yamada K, Murugesan R, Devasahayam N, et al. Evaluation and comparison of pulsed and continuous wave radiofrequency electron paramagnetic resonance techniques for in vivo detection and imaging of free radicals. *J Magn Reson.* 2002;154:287-297.
37. van Nieuw Amerongen GP, van Hinsbergh VW. Cytoskeletal effects of rho-like small guanine nucleotide-binding proteins in the vascular system. *Arterioscler Thromb Vasc Biol.* 2001;21:300-311.
38. Watterson KR, Ratz PH, Spiegel S. The role of sphingosine-1-phosphate in smooth muscle contraction. *Cell Signal.* 2005;17:289-298.
39. Bolz SS, Vogel L, Sollinger D, et al. Nitric oxide-induced decrease in calcium sensitivity of resistance arteries is attributable to activation of the myosin light chain phosphatase and antagonized by the RhoA/Rho kinase pathway. *Circulation.* 2003;107:3081-3087.
40. Coussin F, Scott RH, Wise A, Nixon GF. Comparison of sphingosine 1-phosphate-induced intracellular signaling pathways in vascular smooth muscles: differential role in vasoconstriction. *Circ Res.* 2002;91:151-157.
41. Krishna MC, English S, Yamada K, et al. Overhauser enhanced magnetic resonance imaging for tumor oximetry: coregistration of tumor anatomy and tissue oxygen concentration. *Proc Natl Acad Sci U S A.* 2002;99:2216-2221.
42. Hammond DC, Brooksher RD, Mann RJ, Beerink JH. The dorsal skin-flap model in the rat: factors influencing survival. *Plast Reconstr Surg.* 1993;91:316-321.
43. Mullen MJ, Kharbanda RK, Cross J, et al. Heterogenous nature of flow-mediated dilatation in human conduit arteries in vivo: relevance to endothelial dysfunction in hypercholesterolemia. *Circ Res.* 2001;88:145-151.
44. Khiabani KT, Kerrigan CL. The effects of the nitric oxide donor SIN-1 on ischemia-reperfused cutaneous and myocutaneous flaps. *Plast Reconstr Surg.* 2002;110:169-176.
45. Napoli C, Williams-Ignarro S, de Nigris F, et al. Beneficial effects of concurrent autologous bone marrow cell therapy and metabolic intervention in ischemia-induced angiogenesis in the mouse hindlimb. *Proc Natl Acad Sci U S A.* 2005;102:17202-17206.
46. Knox LK, Angel MF, Gamper T, Amis LR, Morgan RF. Secondary ischemic tolerance improved by administration of L-NAME in rat flaps. *Microsurgery.* 1996;17:425-427.
47. Yu J, deMuinck ED, Zhuang Z, et al. Endothelial nitric oxide synthase is critical for ischemic remodeling, mural cell recruitment, and blood flow reserve. *Proc Natl Acad Sci U S A.* 2005;102:10999-11004.
48. Agah A, Kyriakides TR, Lawler J, Bornstein P. The lack of thrombospondin-1 (TSP1) dictates the course of wound healing in double-TSP1/TSP2-null mice. *Am J Pathol.* 2002;161:831-839.
49. Sorbera L, Bayes M. ABT-510: Oncolytic Angiogenesis Inhibitor. *Drugs Future.* 2005;30:1081-1086.